Appl. Phys. B 76, 473–477 (2003)
DOI: 10.1007/s00340-003-1133-7

Applied Physics B
Lasers and Optics

S. BORRI[1,3]
P. CANCIO[1]
P. DE NATALE[1]
G. GIUSFREDI[1]
D. MAZZOTTI[1,✉]
F. TAMASSIA[2]

Power-boosted difference-frequency source for high-resolution infrared spectroscopy

[1] Istituto Nazionale di Ottica Applicata (INOA), Largo Fermi 6, 50125 Firenze, Italy
[2] Dipartimento di Chimica Fisica e Inorganica – Università di Bologna, Viale del Risorgimento 4, 40136 Bologna, Italy
[3] European Laboratory for Non-linear Spectroscopy (LENS) and Dipartimento di Fisica – Università di Firenze, Via Carrara 1, 50019 Sesto Fiorentino FI, Italy

Received: 19 December 2002/Revised version: 3 February 2003
Published online: 16 April 2003 •

ABSTRACT We analyzed the spectroscopic performance of a difference-frequency source that utilizes a 5-W Yb-fiber amplifier for the "signal" radiation in order to increase the "idler" power generated around 4.3 μm. The amplifier is seeded by a monolithic-cavity Nd:YAG laser at 1064 nm. The intensity noise spectral density of the "idler" radiation was characterized. Cavity-enhanced saturated-absorption spectroscopy was also performed to test the frequency resolution. In particular, we observed the Lamb-dip spectrum of the ro-vibrational $(00^00-00^01)R(0)$ transition of $^{17}O^{12}C^{16}O$ in natural abundance. To our knowledge, this is the first observation of that transition by the Lamb-dip technique.

PACS 42.65.Ky; 07.60.Vg; 42.60.Da; 42.62.Fi; 42.70.Mp; 42.72.Ai; 33.20.Ea

1 Introduction

In recent years, the efficiency of difference-frequency generation (DFG) has largely profited from the field-induced periodically-poling technology of ferro-electric non-linear materials [1] to achieve quasi-phase-matched $\chi^{(2)}$ optical processes. These new photonic devices have been employed in conjunction with diode-pumped solid-state lasers, Er/Yb-fiber amplifiers [2] or semiconductor tapered amplifiers [3] seeded by diode lasers. Some of their most important spectral features, such as frequency stability and tunability, now extend to the mid infrared (IR) spectral region. Applications of these novel DFG-based coherent sources range from trace-gas detection of atmospheric species to high-resolution molecular spectroscopy [4]. Very recently, isotopic ratios, like $^{13}C/^{12}C$ in carbon dioxide, have been accurately measured with a DFG spectrometer [5].

In our laboratory we developed an IR spectrometer based on difference-frequency generation. We first explored the ultimate sensitivity of such devices [6, 7], discovering that such a source is intrinsically almost shot-noise limited at a few kilohertz frequencies, at an "idler" power of few microwatts. However, technical noise like optical fringing and drifts generally limits the actual noise floor in specific spectroscopic applications, although the quantum noise regime can be in principle achieved using appropriate techniques [8]. The low source noise, even at few microwatt power levels, recently allowed us to record sub-Doppler spectra of several transitions in the R-branch of the ν_3 fundamental ro-vibrational band of $^{12}C^{16}O_2$ [9, 10]. Saturation of a large number of IR transitions for many molecular species (e.g. CO_2, CO, N_2O, CH_4) allows us to build an accurate "comb" of reference frequencies [11]. Until now, we have been working on the fundamental transitions of CO_2 around 4.25 μm, that have been saturated with a power as low as a few microwatts. To extend the range of saturable transitions, a higher "idler" power is needed. In fact, under the same experimental conditions (pressure, beam waist, ...) the saturation intensity is proportional to the inverse squared dipole moment of the transition and can be significantly higher (e.g. one order of magnitude or more for the fundamental ro-vibrational bands of CO and CH_4) than the CO_2 value (about 10 mW/mm^2). Even Lamb-dip spectra of transitions with a relatively low saturation threshold may represent a serious challenge, due to the "idler" absorption by the wings of nearby strong transitions. Therefore, in order to obtain a higher "idler" power, we set up a power-boosted difference-frequency spectrometer, that amplifies "signal" radiation from a monolithic Nd:YAG laser around 1064 nm up to 5 W. A detailed characterization of this source was carried out, in order to test its suitability for sub-Doppler and high-sensitivity spectroscopy.

2 Experimental setup

The optical setup for our experiment is shown in Fig. 1. To enhance the "idler" power, we amplified the "signal" laser by inserting a commercial double-stage Yb-fiber amplifier (IPG Photonics, mod. YAM-5) in the setup described in [10]. This amplifier delivers up to 5 W optical power around 1064 nm at an input power > 1 mW. The amplifier architecture was optimized to avoid stimulated Brillouin scattering when seeded with a narrow-linewidth (kilohertz) laser, as our monolithic-cavity Nd:YAG. We injected the amplifier with a few tens of milliwatts from the Nd:YAG laser. The amplified "signal" is collimated by a high-power output coupler to a 1.6 mm diameter

✉ Fax: +39-055/4572-451, E-mail: mazzotti@inoa.it

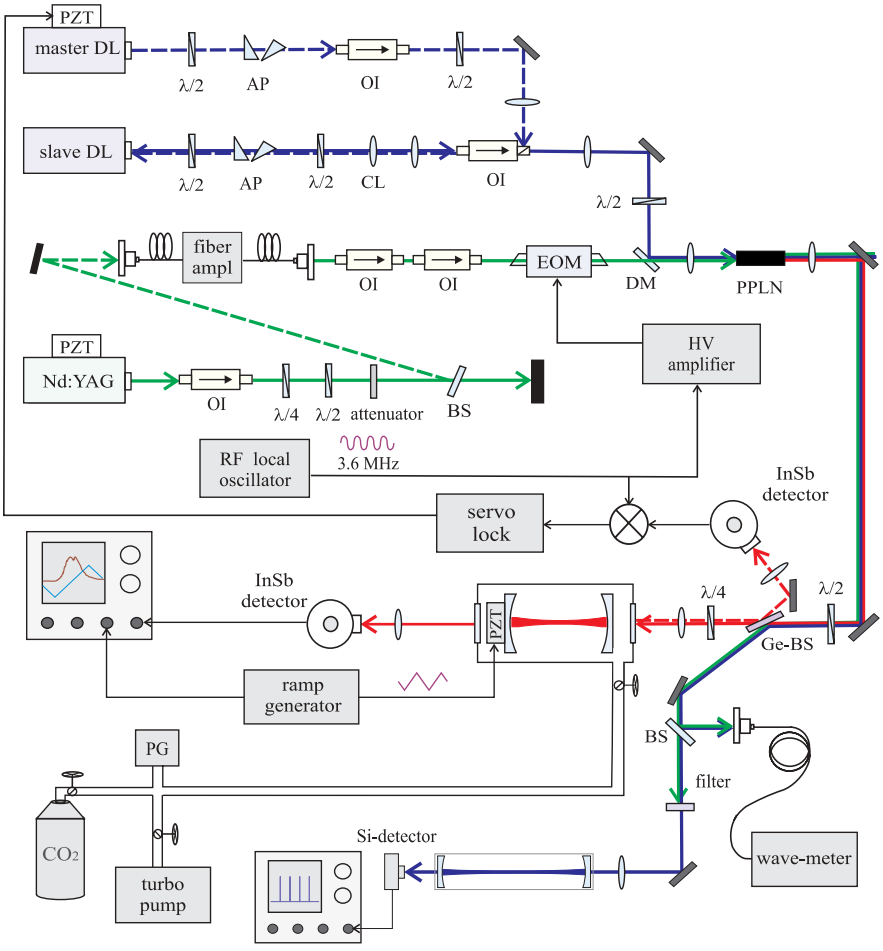

FIGURE 1 Optical scheme of the experimental setup. Legend: PZT → piezo-electric translator; OI → optical isolator; λ/2, λ/4 → half-wave, quarter-wave plates; AP → anamorphic prisms; CL → cylindrical lens; EOM → electro-optic phase modulator; DM → dichroic mirror; PPLN → periodically-poled $LiNbO_3$ crystal (length $l = 40$ mm, width $= 5$ mm, thickness $= 0.5$ mm, poling period $\Lambda = 23.0$ μm); BS → beam–splitter; PG → pressure gauge. The two identical liquid-N_2-cooled InSb photodiodes have a responsivity of about 2.8 A/W and a frequency bandwidth of about 5 MHz

and is about 7 times more powerful than the maximum Nd:YAG power. The "pump" beam is delivered by the master/slave diode laser system, as in the previous setup [10]. The laser tuning ranges are 1064.45–1064.55 nm for the Nd:YAG and 848–855 nm for the master/slave diode laser system. The master diode laser tuning range is limited to only about 7 nm, because there is no anti-reflection (AR) coating on the laser output facet. The corresponding "idler" wavelength range is about 4.15–4.35 μm.

An attenuator and a combination of a half-wave and a quarter-wave plate are placed before the input fiber port. The plates are rotated to compensate the natural fiber–amplifier birefringence, in order to get a *p*-polarized beam at the output of the fiber collimator. The amplified beam becomes *s*-polarized after two optical isolators, as required by the orientation of the non-linear crystal optical axis. This pair of isolators at the amplifier output is required to ensure a minimum 50 dB isolation, to avoid possible damage to the amplifier due to unwanted optical feedback. Similarly, the attenuator is required to avoid damage to the pre-amplification stage of the amplifier.

The IR generated radiation is coupled to a resonant confocal optical cavity as described in Ref. [10], in order to perform high-resolution saturated-absorption spectroscopy. The concave mirrors spacing (and radius of curvature) is 115 mm, corresponding to a free spectral range of about 1.3 GHz. Their reflectivity of about 99.5% (calculated from a measured optical finesse of about 550) gives a power buildup factor of about 200 and an effective absorption path of about 40 m. This is a good compromise between a high enough intra-cavity intensity and a not too narrow resonance width (causing possible coupling and locking troubles). In the present setup, however, both the radiation power coupled to the cavity and that reflected from it (used for locking the master diode laser to the cavity resonance with the Pound–Drever–Hall scheme [12]) has been increased by introducing a half-wave and a quarter-wave plate and a Ge beam-splitter at the Brewster angle (about 74°) after the non-linear crystal. Moreover, the dominant interference fringes between the cavity input mirror and the crystal output facet (with an imperfect AR coating) are strongly suppressed (by about a factor of 100) by the round-trip polarization crossing effect of the plates.

3 Measurements

3.1 *Efficiency*

With this setup, we first measured the "idler" power generated in the non-linear crystal vs. the "signal" power provided by the injected Yb-fiber amplifier. The results are shown in Fig. 2. About 30% of the "signal" power is lost through the two optical isolators and the electro-optic modulator. The generated "idler" power grows linearly with the effective "signal" power, as expected. With the fiber amplifier operated at its maximum gain, corresponding to a "signal" power incident onto the crystal of 3.83 W, and 78 mW incident "pump" power, we measured up to 172 μW "idler" power. Taking into account a loss of 5% due to the imperfect AR coating on the crystal facets, affecting the "pump" and "signal" input beams and the "idler" output beam, we can estimate a maximum efficiency of $1.7 \times 10^{-2}\,\mathrm{W^{-1}m^{-1}}$ for the DFG process.

The expression for the "idler" power generated in an absorbing non-linear crystal with a DGF process can be derived by generalizing Chu and Broyer's theory [13]. The result is:

$$P_\mathrm{i} = P_\mathrm{p} P_\mathrm{s} \frac{32\pi^2 d_\mathrm{eff}^2 l}{\varepsilon_0 c n_\mathrm{i} \lambda_\mathrm{i}^2 \left(n_\mathrm{s}\lambda_\mathrm{p} + n_\mathrm{p}\lambda_\mathrm{s}\right)} \times h(\xi, \sigma, \mu, \alpha, l) \quad (1)$$

where d_eff is the effective non-linear coefficient, l is the crystal length, P is the

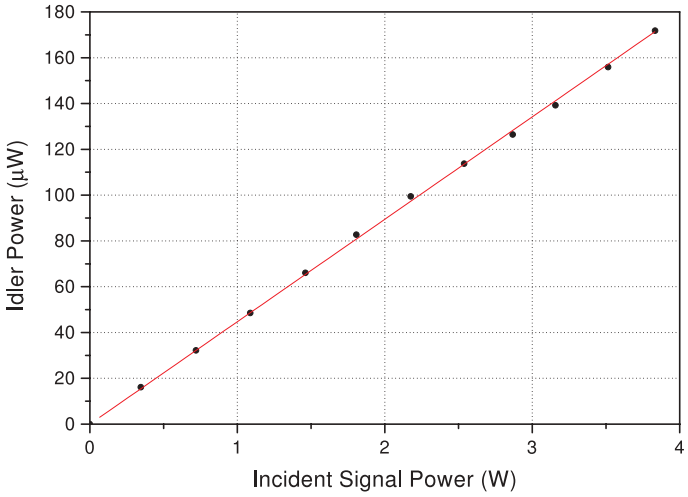

FIGURE 2 Dependence of the generated "idler" power on the incident "signal" power. The incident "pump" power is fixed to 78 mW. A linear fit of the data points is also shown

power, λ is the wavelength, n is the refraction index and the subscripts p, s, i refer to "pump", "signal" and "idler", respectively. The focusing function h is defined as:

$$h(\xi,\sigma,\mu,\alpha,l) \equiv \frac{\mathrm{e}^{-\frac{\alpha l}{2}}}{4\xi} \times \int_{-\xi}^{\xi} \mathrm{d}\tau \int_{-\xi}^{\xi} \mathrm{d}\tau' \, \mathrm{e}^{-\mathrm{i}\sigma(\tau-\tau')+\frac{\alpha l}{4\xi}(\tau+\tau')} \times \frac{1}{1+\tau\tau'-\mathrm{i}\frac{1+\mu^2}{1-\mu^2}(\tau-\tau')} \qquad (2)$$

where

$$\xi \equiv \frac{l}{b}, \quad \mu \equiv \frac{n_\mathrm{s}\lambda_\mathrm{p}}{n_\mathrm{p}\lambda_\mathrm{s}},$$
$$\sigma \equiv -\pi b\left(\frac{n_\mathrm{p}}{\lambda_\mathrm{p}} - \frac{n_\mathrm{s}}{\lambda_\mathrm{s}} - \frac{n_\mathrm{i}}{\lambda_\mathrm{i}} - \frac{1}{\Lambda}\right) \qquad (3)$$

α is the absorption coefficient, b is the confocal parameter of both "pump" and "signal" beams. A numerical calculation of h with $\alpha = 0.24\,\mathrm{cm}^{-1}$ [14], $\mu = 0.795$ gives a maximum value $h_\mathrm{max} \approx 0.26$ for $\xi_\mathrm{opt} \approx 2.2$ and $\sigma_\mathrm{opt} \approx 0.9$. Taking $d_\mathrm{eff} = 14\,\mathrm{pm/V}$, the maximum calculated power is about 470 μW. Therefore our experimental efficiency is about 36% of the theoretical value. This value is comparable with typically achieved conversion efficiencies in similar setups, whereas higher values can be obtained using fiber-optic coupling [2].

3.2 *Noise*

We measured the intensity–noise spectrum of the "idler" radiation at different amplified "signal" power levels. The results are shown in Fig. 3. The calculated "idler" shot-noise level corresponding to 1.9 W "signal" power is also plotted. It can be observed that the shot-noise level is approached above 1.4 MHz frequency. The shape of these spectra traces well the Nd:YAG laser intensity noise. The relaxation-oscillation noise peak at about 800 kHz is reduced by noise-eater feedback electronics. In order to estimate the "idler" noise contribution from the fiber amplifier, we show in Fig. 3 two curves corresponding to the "idler" noise spectral density with amplified and non-amplified Nd:YAG radiation at the same power. The curves are almost overlapping and the maximum difference between them is about 1.5 dB, around 800 kHz frequency.

In order to estimate the amount of technical noise, we measured the noise power in the 200–400 kHz frequency region. We averaged the intensity noise in this frequency interval and the results are shown in Fig. 4. Each point is the average of 40 nearby values. The data points were fitted to the theoretical curve [6]:

$$N = a_0 + a_1 I + a_2 I^2 \qquad (4)$$

where I is the detected photocurrent and N is the current noise spectral density. The first term accounts for the thermal background and for the preamplifier electronics: $a_0 = 2eI_\mathrm{b} + N_\mathrm{el}$. The linear term $a_1 I$ is the shot-noise contribution. The quadratic term $a_2 I^2$ accounts for technical noise. We fitted the experimental data to this quadratic curve keeping the linear term a_1 fixed to its theoretical value $2e$. The electronic noise N_el from the preamplifier is dominant with respect to the thermal background noise $2eI_\mathrm{b}$. The noise parameter a_2 is slightly smaller than that measured in Ref. [6] in the 2–5 kHz frequency region, due to the reduced $1/f$ noise in the 200–400 kHz range. The dominant source of the technical noise are the Nd:YAG amplitude fluctuations.

3.3 CO_2 *spectra*

In order to test the frequency resolution of this apparatus, we observed

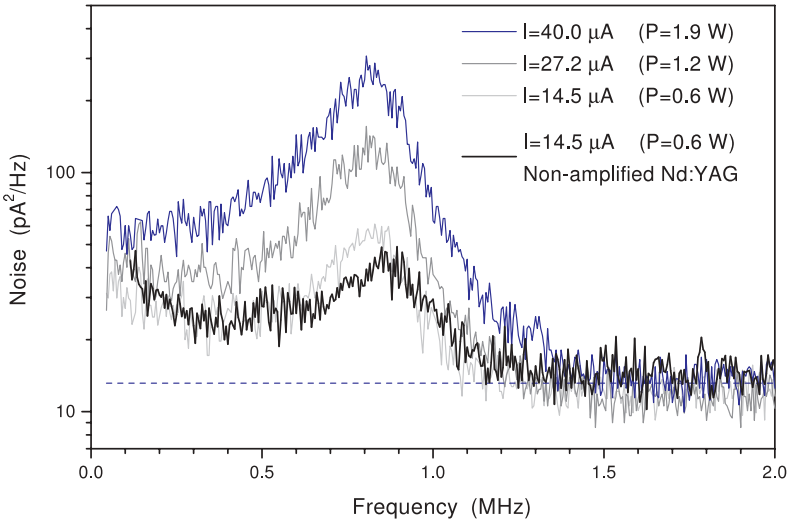

FIGURE 3 "Idler" noise spectral density at different amplifier output powers P. The spectrum analyzer parameters are: 10 kHz resolution bandwidth, 16 s acquisition time, 3 MHz frequency span. The reported I values correspond to the detector photocurrent

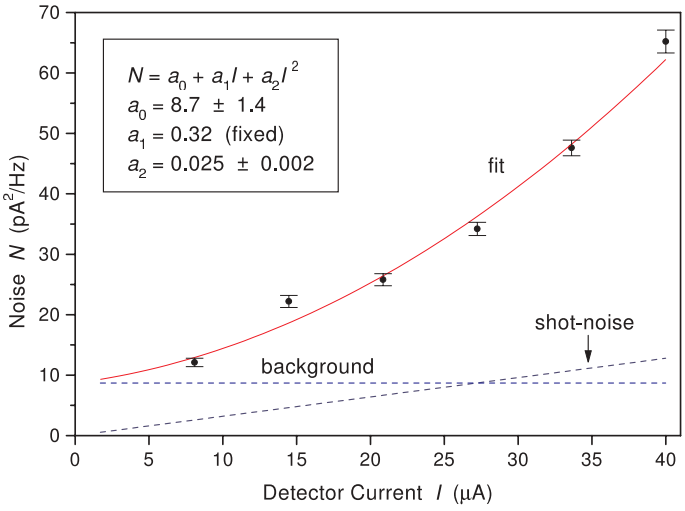

FIGURE 4 Noise density vs. "idler" power (reported as detector photocurrent) fitted to a parabolic curve. The *dashed lines* are the calculated shot-noise level and background noise

the saturated ro-vibrational $(00^00-00^01)R(0)$ transition of $^{17}O^{12}C^{16}O$ in natural abundance (0.076%). This isotopomer exhibits an electric-quadrupole hyperfine structure due to the coupling of the electric-field gradient with the ^{17}O nuclear spin ($I = 5/2$) [15, 16]. This is the best suited transition for our test, because it has got the widest hyperfine separation with the minimum number of components. In Ref. [16] the $J = 1 - 0$ ground state pure rotational transition of $^{17}O^{12}C^{16}O$ was detected by Fourier transform microwave spectroscopy and the electric-quadrupole coupling constant eqQ was determined as $-3.92(9)$ MHz [16]. The frequency shifts $\Delta\nu$ and fractional intensities w calculated for the 3 hyperfine components [17] are shown in Table 1. The total width of the multiplet is only 1.18 MHz.

On the other hand, this CO_2 isotopomer is a convenient candidate for testing the improved saturation capabilities when the "idler" power is strongly attenuated in air. In fact, the strongest $^{17}O^{12}C^{16}O$ ro-vibrational lines are coincident with the fundamental ro-vibrational $(00^00–00^01)$ pressure-broadened transitions of the most abundant isotopomer $^{12}C^{16}O_2$. Because of this overlap our previous attempts to record this saturated transition using our low-power setup [10] failed, even if most of the path was purged with nitrogen. This absorption by CO_2 affects not only the radiation power coupled to the cavity, but also the stability of the locking-loop error signal. Indeed, a worse compensation of relative fluctuations between the radiation frequency and the cavity resonance leads to a larger contribution to the intensity noise of the transmitted signal. In order to reduce such noise, we combined the transmission and reflection signals, adding each other with appropriate weights. As they are both affected by the same technical intensity noise, this can be largely reduced without any significant signal reduction. We can state that the overall effect is an increase of the signal-to-noise (S/N) ratio on the dip from less than 1 to about 5.

Figure 5 shows a sub-Doppler recording of the $R(0)$ line. The experimental data can be fitted to a theoretical curve of the saturated-absorption coefficient [18], assuming a Lorentzian-shaped dip and the saturation parameter $I/I_S \ll 1$, where I_S is the saturation intensity. This latter assumption is justified, since the value of that ratio obtained from the fit is 0.151(17). The corresponding contrast ratio is about 8%. The Lorentzian width (FWHM) of the Lamb-dip is 2.7(5) MHz. The estimated contributions to the experimental width (FWHM) are about 1.2 MHz for pressure broadening and 380 kHz for transit-time broadening. Considering the additional broadening due to the hyperfine splitting, we can reasonably estimate that the radiation linewidth is at most a few hundred kilohertz over a millisecond time scale, i.e. about the same linewidth we had without the fiber amplifier. We had already obtained a similar result by analyzing the noise characteristics of a 1-W Yb-fiber amplifier at 1083 nm [19]. The hyperfine structure could not be resolved, primarily because of the CO_2 pressure broadening and secondarily because of the instrumental resolution limited by the laser linewidth and the transit-time broadening. However, even at lower pressures we did not observe a substantial resolution improvement, because of the significant worsening of the S/N ratio.

The main contribution to the observed noise of the spectrum in Fig. 5 does not depend on the source noise measured in Sect. 3.2, but arises from residual cavity-radiation frequency fluctuations and optical fringes. Other

F'	$\Delta\nu$ (MHz)	w
3/2	0.55	0.22
5/2	−0.63	0.33
7/2	0.20	0.44

TABLE 1 Calculated hyperfine structure for the $(00^00-00^01)R(0)$ $F = 5/2 \rightarrow F'$ transition of $^{17}O^{12}C^{16}O$

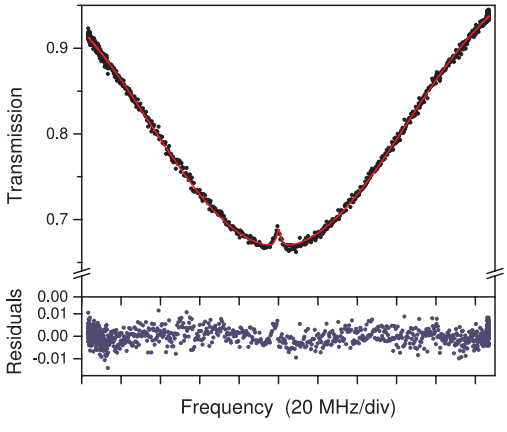

FIGURE 5 Ro-vibrational (00^00-00^01) $R(0)$ saturated line of $^{17}O^{12}C^{16}O$ at 2340.765 cm^{-1}. The experimental points correspond to 31 averaged acquisitions taken at a rate of 3 Hz. The CO_2 pressure is 27 Pa. The incident "signal" power is 1.4 W. The detected power is about 1 μW. The fit curve and residuals are also shown.

spectroscopic techniques [20, 21] can efficiently reduce the technical noise, thus allowing us to approach the quantum-limited source noise.

4 Summary

In conclusion, this work has demonstrated that our fiber-amplified DFG spectrometer has the suitable features for high-sensitivity and high-resolution spectroscopy around 4.3 μm wavelength. In fact, we have shown that the "idler" intensity noise, when using the Yb-fiber amplifier, increases by less than 1.5 dB, whereas the estimated radiation linewidth does not exceed a few hundred kilohertz (over a millisecond timescale), thus allowing to perform Lamb-dip spectroscopy.

ACKNOWLEDGEMENTS We wish to thank Prof. G. Di Lonardo (University of Bologna, Italy) for helpful discussions about the hyperfine structure of $^{17}O^{12}C^{16}O$ and Dr. R.E. Drullinger (National Institute of Standards and Technology, USA) for a critical reading of the manuscript. This work was partly supported by Gruppo Nazionale per la Vulcanologia (GNV).

REFERENCES

1 M. Yamada, N. Nada, M. Saitoh, K. Watanabe: Appl. Phys. Lett. **62**, 435 (1993)
2 D. Richter, A. Fried, B.P. Wert, J.G. Walega, F.K. Tittel: Appl. Phys. B **75**, 281 (2002)
3 K.P. Petrov, L.W. Goldberg, W.K. Burns, R.F. Curl, F.K. Tittel: Opt. Lett. **21**, 86 (1996)
4 D. Mazzotti, G. Giusfredi, P. Cancio, P. De Natale: Opt. and Lasers in Eng. **37**, 143 (2002)
5 M. Erdelyi, D. Richter, F.K. Tittel: Appl. Phys. B **75**, 289 (2002)
6 D. Mazzotti, P. De Natale, G. Giusfredi, C. Fort, J.A. Mitchell, L.W. Hollberg: Appl. Phys. B **70**, 747 (2000)
7 P. De Natale, D. Mazzotti, G. Giusfredi, J.A. Mitchell, L.W. Hollberg: in L.W. Hollberg, R.J. Lang (Eds.), *Advanced Semiconductor Lasers and Their Applications 1999*, Vol. 31, Trends in Optics and Photonics Series (Optical Society of America, Washington DC, 2000) p. 122
8 J. Ye, L.S. Ma, J.L. Hall: J. Opt. Soc. Am. B **15**, 6 (1998)
9 D. Mazzotti, P. De Natale, G. Giusfredi, C. Fort, J.A. Mitchell, L.W. Hollberg: Opt. Lett. **25**, 350 (2000)
10 D. Mazzotti, S. Borri, P. Cancio, G. Giusfredi, P. De Natale: Opt. Lett. **27**, 1256 (2002)
11 S. Borri, P. Cancio, G. Giusfredi, D. Mazzotti, P. De Natale: in *Proceedings of Conference on Lasers, Applications and Technologies (LAT 2002)*, Vol. xxx, SPIE Proceedings, (SPIE) in press.
12 R.W.P. Drever, J.L. Hall, F.V. Kowalski, J. Hough, G.M. Ford, A.J. Munley, H. Ward: Appl. Phys. B **31**, 97 (1983)
13 T.-B.-Chu, M. Broyer: J. Physique **45**, 1599 (1984)
14 L.E. Myers, R.C. Eckardt, M.M. Fejer, R.L. Byer: Opt. Lett. **21**, 591 (1996)
15 R. Eggenberger, S. Gerber, H. Huber, D. Searles, M. Welker: J. Mol. Spectrosc. **151**, 474 (1992)
16 J. Gripp, H. Mäder, H. Dreizler, J.L. Teffo: J. Mol. Spectrosc. **172**, 430 (1995)
17 C.H. Townes, A.L. Schawlow, *Microwave spectroscopy*, (Dover Publications, New York, 1975) p. 504
18 V.S. Letokhov, V.P. Chebotayev, *Non-linear laser spectroscopy*, (Springer-Verlag, Berlin, 1977) p. 59
19 P. Cancio, P. Zeppini, P. De Natale, S. Taccheo, P. Laporta: Appl. Phys. B **70**, 763 (2000)
20 J. Ye, J.L. Hall: Phys. Rev. A **61**, 061 802(R) (2002)
21 G. Modugno, C. Corsi, M. Gabrysch, F. Marin, M. Inguscio: Appl. Phys. B **67**, 289 (1998)